

Design and Analysis of a High-Powered Rocket Airbrake System

Neil Sanipara^{*}, Alex Belew[†], Tyler Sprague[‡]
Mississippi State University, Mississippi State, MS, 39762, USA

The Space Cowboys are Mississippi State University's high-powered rocketry design team which competes annually at the Spaceport America Cup. A significant portion of scoring at the event is achieving an accurate flight apogee according to the category of competition. This paper presents the design and evaluation of a prototype airbrake system that utilizes extendable surfaces to control rocket apogee during coast phase. An aerodynamic analysis was performed by using analytical calculations, semi-empirical software tools, and a CFD simulation. A closed-loop feedback system utilizing an optimal controller scheme is implemented for path-planning and control of the rocket trajectory during ascent. The system is then verified and validated using a 6-DOF simulation of a high-powered rocket. The results of these analyses sufficiently prove that this system is effective in controlling apogee during ascent and can be implemented on a future Space Cowboys competition rocket.

I. Nomenclature

A	=	Cross-sectional area, in ²
C_d	=	Coefficient of drag
D_a	=	Drag after deployment of fins
D_b	=	Drag before deployment of fins
F_a	=	Airbrake Force
F_d	=	Drag force, lbf
L	=	Angular Torque
V_k	=	Velocity Vector
x_{CG}	=	Location of center of gravity, in
x_{CP}	=	Location of center of pressure, in
X_o	=	Initial rocket state
X_f	=	Final rocket state
Z_k	=	Position Vector
α	=	Angle-of-Attack, degrees
Ω_k	=	Euler Angle Vector
ρ	=	Density (of atmosphere), slugs/ft ³
v	=	Velocity, ft/s

II. Introduction

THE Space Cowboys rocketry team at Mississippi State university designs and builds a high-powered rocket for the Spaceport America Cup, an annual rocketry competition that takes place in Las Cruces, New Mexico. The competition awards nearly a third of a team's points based on the over-performance or under-performance of their rocket's apogee, according to their competition category. Since so much emphasis is placed on teams hitting their target altitudes, various strategies have been employed by teams to reduce their margins of error. One such strategy has been the development and use of airbrakes¹. This senior seminar project aims to design and analyze the performance of a high-powered rocket airbrake system prototype.

^{*} Student, Department of Aerospace Engineering, AIAA Student Member (ID 1344102), Undergraduate Team.

[†] Student, Department of Aerospace Engineering, AIAA Student Member (ID 1604892), Undergraduate Team.

[‡] Student, Department of Aerospace Engineering, AIAA Student Member (ID 1387492), Undergraduate Team.

An airbrake system is a form of an active control system that can be utilized to decrease the energy of the rocket during flight by employing drag-inducing fins that can extend out from the rocket body. The system is responsible for strategically slowing down the rocket’s velocity during the coasting phase to achieve the specific altitude target. This requires that the system keeps the rocket stable during flight, has a very low response time for its control system, and produces enough drag to tangibly influence the trajectory of the rocket.

The following sections describe the design process for the physical airbrake mechanism, the control system, the process for characterizing aerodynamic properties, and analysis of the performance of the airbrake system using a flight simulation program. If the designed prototype meets all specified requirements, this system may be scaled and implemented into a hybrid rocket being developed for the 2024-2025 Space Cowboys competition year.

III. Design Process

The overall design for the airbrake system is primarily dictated by the mass and stability characteristics of the launch vehicle. A rocket with a larger mass has greater inertia at comparable speeds, requiring more drag to slow the vehicle down. The prototype developed by this project was initially designed to fit the Space Cowboys’ 2023-2024 research vehicle planned to fly in the spring of 2024. However, scheduling constraints in the research vehicle’s manufacturing has required the use of a Level 2 (L2) certification rocket to verify the system. While considered a setback at first, this allowed the team to test the system's scalability as the airframe diameter is reduced from six inches to four. An OpenRocket model of the L2 rocket being used is seen below in Fig. 1. The vehicle is 84 in. in length with an outer diameter of 4.12 in. and weighs 11.3 lbs. with propellant loaded. It has a simulated apogee of 4,157 feet, traveling at a top speed of 566 ft/s, or Mach 0.509. Integrating into the vehicle, the airbrake system is composed of three parts: a 4-inch structural coupler that houses the mechanism and slides into the other airframe tubes, a compact fin-mechanism that minimizes the volume required, and an independent controller that actuates the airbrake surfaces.

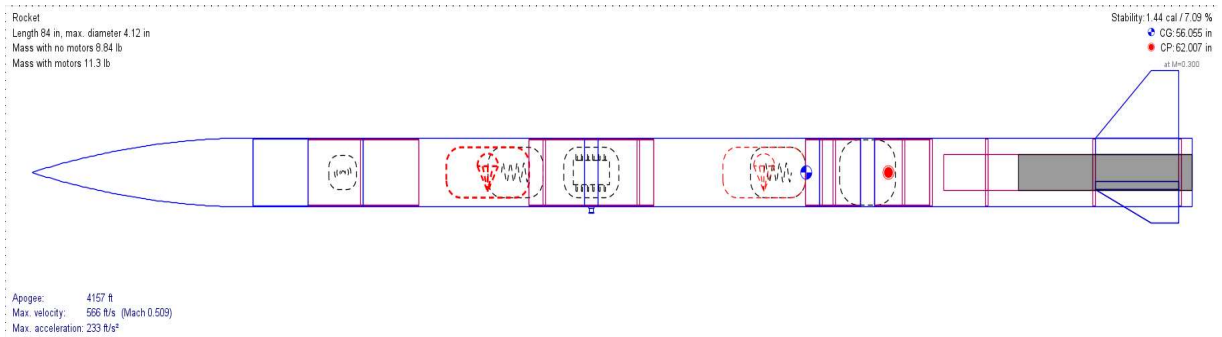


Figure 1. Model of the L2 certification launch vehicle.

A critical factor in determining the performance of a launch vehicle is the stability factor⁴. Stability is dictated by the relative locations of the center of pressure (CP) and center of gravity (CG) of the vehicle using Eq. (1).

$$stability = \frac{x_{CG} - x_{CP}}{airframe\ diameter} \quad (1)$$

The center of pressure is the point at which all the aerodynamic forces (lift, drag, moments) act. To keep the rocket stable in flight, the center of gravity must remain forward of the aerodynamic center of pressure. Any type of protrusion on the rocket body can create a high-pressure region, shifting the center of pressure in the direction of the protrusion. This is the reason fins are typically added to rockets, to shift the CP towards the tail of the rocket (further from CG). The airbrake system prototype is chosen to be placed behind the center of gravity on the flight vehicle to minimize instability during the rocket’s flight.

A. Mechanical Design

The mechanical design of the airbrake system's fin extension mechanism plays an important role in the responsiveness and practicality of the system. The fin mechanism is responsible for the deployment and structural support of the airbrake's fins. The fins undergo extreme bending loads due to the high-pressure produced at the front of the fin by the fast-moving air. This load must be carried by the mechanism itself. In addition, the mechanism must be able to symmetrically deploy the fins from the rocket body to prevent asymmetrical drag, which can cause instability during the rocket's flight. Teams at the Spaceport competition have typically used a gear or linkage system to deploy the fins outwards from slots cut into the body of the rocket⁴.

The design chosen for this project was a rack and pinion system that deploys the fins via a rotation of a central shaft. This was primarily due to the ease of prototyping using additive manufacturing. One of the two joints is constrained to move via a channel cut into the surface that the fin rests on. This mechanism was housed in a 4-inch coupler to support integration into the launch vehicle via threaded rods. This design is shown in Fig. 3 below.

A 35 kg-cm high-torque servo was chosen to drive the central shaft of the system to prevent binding issues that could occur due to the high-loads applied to the fins. As the central shaft rotates, the fins are deployed to full extension. This system will be tested before integration into the launch vehicle. A figure showing the full extension of the airbrake system is shown below.

B. Fin Design

The fins of the airbrake system act as the drag-generating entities to lower the rocket's velocity during flight. The amount of drag produced varies as a function of the total surface area of the extended fins, speed of the rocket, and the angle of attack during flight.

The fin design that was created was chosen to maximize the drag produced by the airbrake system through the total surface area while also minimizing the impact to the structural integrity of the rocket's airframe. The design chosen was a square-shaped fin with a curved edge to fit the profile cutouts on the airbrake coupler that matched the outer diameter of the airframe. This design allows for slot cut-outs that only take away half of the airframe circumference for greater structural integrity while simplifying the aerodynamic calculations required due to the simplified shape. The design of the airbrake fins is shown in Fig. 4. A total of four fins were chosen to produce a symmetrical drag profile about the rocket's cross-section.

C. Control System Hardware Design

The control system of the airbrake system must have a low-response time due to the short ascent duration of a high-powered rocket. The system must be able to process the velocity, position, and acceleration of the rocket at each point during the flight to estimate the trajectory of the rocket and actuate the fins at an appropriate extension setting to apply the appropriate amount of drag.

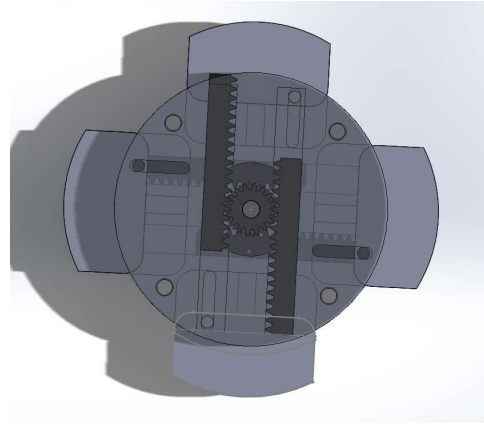


Figure 2. Deployed configuration of airbrakes.

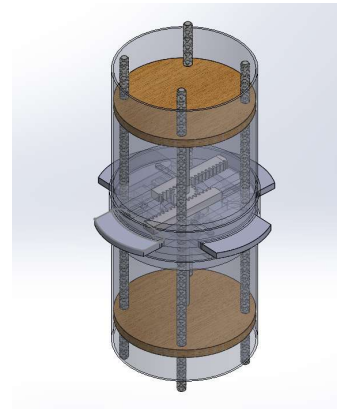


Figure 3. Model of the airbrake system prototype.

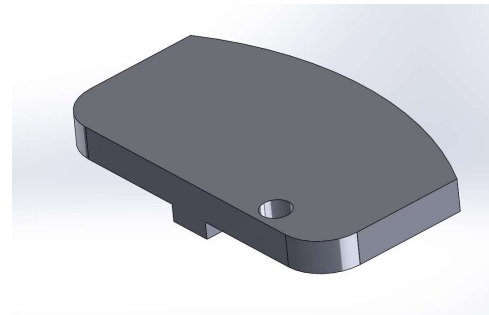


Figure 4. Single airbrake fin.

The first iteration of the airbrake system controller consists of a proportional–integral–derivative (PID) controller for actuating the 4 fin-surfaces simultaneously according to a set drag-profile during flight. The sensor data is collected and filtered using the Pixhawk quadcopter flight controller platform. This system is still a work in progress.

IV. Aerodynamic Analysis

A. Aerodynamic Characterization

1. Analytical Calculations

To reach a specified apogee, the airbrake system's drag characteristics after fin deployment, D_a , are crucial for the control system. The drag calculation before fin deployment, D_b , is determined using the Ras Aero II software. Once D_b is obtained, the drag on the fins can be calculated using the bluff body C_d approximation of 1.28 for a flat plate⁴. There are four fins, each with a surface area of 1.55 in², resulting in a total surface area of 6.2 in². During flight, the rocket experiences a drag value of 19.428 lbs. at a speed of 578 ft/s. When deployed, the fins generate a drag value of approximately 17 lbs. Using hand calculations, the total drag after airbrake deployment is around 36 lbs. while the Ras Aero II software predicts the total drag to be around 32 lbs.

The drag calculations were computed in MATLAB over a range of velocities, altitudes, and angles of attack. The resulting 4D data set creates a lookup table in which the implemented control system can reference. This allows us to determine the deployment surface area needed for a given altitude and velocity. Figure 5 shows the resulting data.

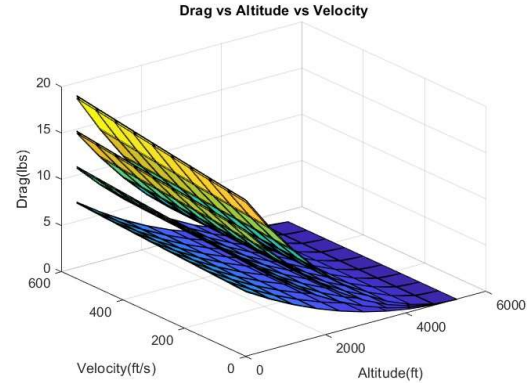


Figure 5. Analytical calculation results of drag vs. altitude vs. velocity.

2. Computational Fluid Dynamics

To get a better understanding of the range of drag forces the rocket may see during flight, Computational Fluid Dynamics (CFD) simulations were used to verify analytical calculations. For our purposes, SolidWorks Flow Simulation was used after modeling the rocket body in SolidWorks. Using set airspeed and atmospheric conditions, the program can estimate the axial forces experienced by the rocket. An additional equation goal was set to calculate during the simulations, which backed out the coefficient of drag by solving for C_d in Eq. (2).

$$F_d = \frac{1}{2} \rho v^2 C_d A \quad (2)$$

The drag force and corresponding C_d value were simulated first on the rocket without any drag altering surfaces. Since the predicted altitude of the L2 rocket is relatively low, a few test cases were run to see how much the atmospheric conditions affected the drag quantities. A test case with the rocket without fins with a velocity of around 650 ft/s (faster than the predicted top speed) gave a drag force of 17.57 lbs. and a C_d of 0.4235 in 2,500 ft atmosphere conditions. The same simulation was run with atmospheric conditions set to 4,500 ft values, resulting in a drag force of 16.57 lbs. and a C_d of .4243. The difference between the two cases is only 1.0 lbs., roughly 5.7%, so it was determined that with the small range of altitudes, the differences due to atmospheric conditions were negligible to simplify computations. Therefore, unless noted, the rest of the simulations were run with atmospheric conditions set to 4,000 feet. The following figure shows the simulated flows of the rocket near top predicted speed of 650 ft/s.

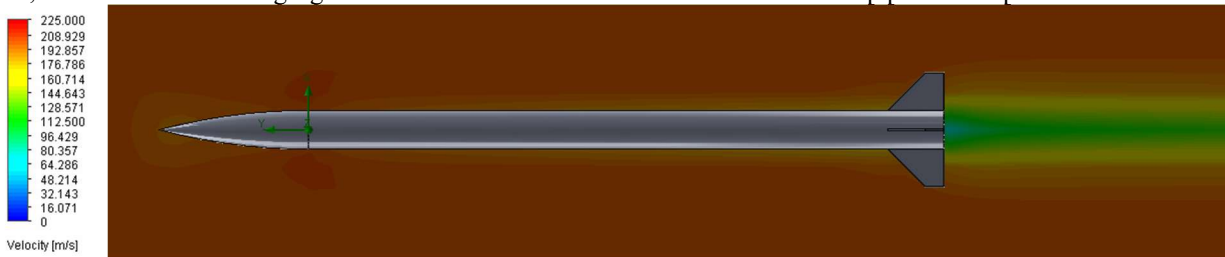


Figure 6. Velocity gradient over brakeless rocket body at 650 ft/s.

The brakeless rocket was then put through a variety of simulations to characterize drag at different airspeeds. Sweeping through 0 ft/s through ~738 ft/s (well above predicted top speed but accounting for variability in motor performance) at increments of just over 82 ft/s. The airbrakes were then added to the model, on the vehicle, and simulated at quarter, half, three-quarters, and full fin deployment. Full results from these simulations are presented in Appendix A. The important information to pull from this data is the effect that the braking surfaces have on the forces of the vehicle, which can be seen in the following table.

Table 1. Drag forces and comparisons between brakeless rocket and 25%, 50%, 75%, and 100% deployment.

Velocity (ft/s)	F _d (lbf) @ 0% Deploy	F _d (lbf) @ 100% Deploy	ΔF _d @ 100%	F _d (lbf) @ 75% Deploy	ΔF _d @ 75%	F _d (lbf) @ 50% Deploy	ΔF _d @ 50%	F _d (lbf) @ 25% Deploy	ΔF _d @ 25%
0	0	0	0	0	0	0	0	0	0
82.025	0.2738	0.4167	0.1430	0.3499	0.0761	0.2740	0.0002	0.2658	-0.0080
164.050	1.1315	1.6960	0.5646	1.4302	0.2987	1.1363	0.0048	1.1072	-0.0243
246.075	2.4684	3.7457	1.2773	3.1445	0.6761	2.4830	0.0145	2.4081	-0.0603
328.100	4.2938	6.5668	2.2729	5.5006	1.2068	4.3191	0.0252	4.1856	-0.1082
410.125	6.6012	10.1775	3.5763	8.5316	1.9304	6.6374	0.0362	6.4878	-0.1133
492.150	9.3855	14.5816	5.1961	12.2007	2.8152	9.4511	0.0656	9.2768	-0.1087
574.175	12.5971	19.6894	7.0923	16.4946	3.8975	12.7094	0.1123	12.4746	-0.1225
656.200	16.3470	25.4868	9.1398	21.4077	5.0606	16.4473	0.1002	16.2790	-0.0680
738.225	20.4817	31.9033	11.4216	26.8231	6.3414	20.5959	0.1142	20.4567	-0.0250

The additional drag induced by the airbrake fins are quite low for the 25% and 50% deployment states. While they won't be ignored completely during implementation of the actual system and its control, those results will be ignored in the following graph in Fig. 7 that shows the vehicles drag over velocity at 0%, 75%, and 100% deployment. The delta force between the 100% and 0% states are also graphed. It can be determined at a quick glance that a significant increase in drag can be attributed to the airbrake system.

A final comparison being drawn between the various states of deployment concerns the coefficient of drag. A coefficient of drag vs. Mach number is a common aerodynamic visual for

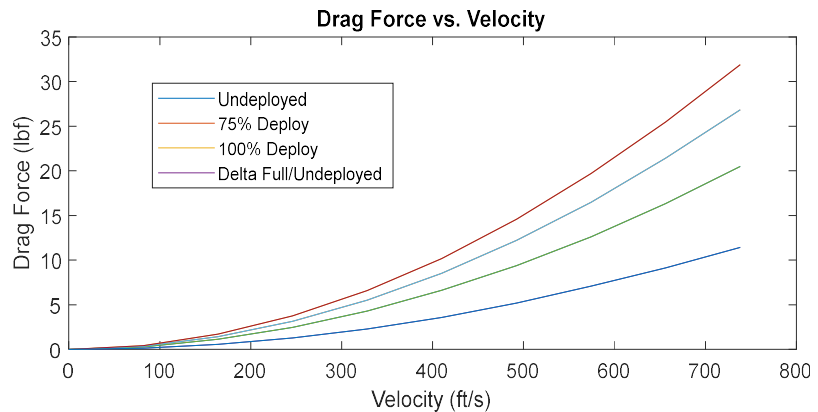


Figure 7. Drag force plotted against velocity at 0%, 75%, and 100% airbrake deployment.

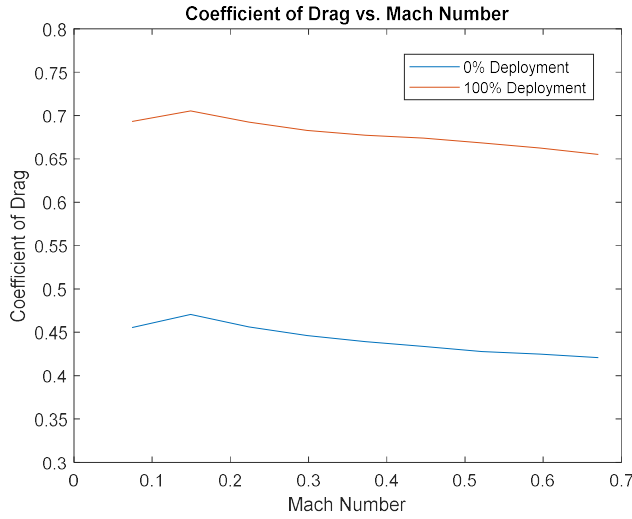


Figure 8. Coefficient of drag values for no deployment and full deployment of airbrakes.

simulation of a 6-DoF dynamic model of the rocket in conjunction with an optimal controller was utilized to analyze the response of the airbrake system to common flight disturbances, such as wind¹.

A. Dynamics Model

The dynamics of a high-powered rocket can be described using a 12-dimensional state vector describing the 6-DoF of the system³, described in the appendix in Appendix B. Reference values for aerodynamic coefficients such as base-drag and coefficient of axial force was computed for the L2 rocket using the semi-empirical aerodynamic software RAS Aero II⁹. A set of simplifying assumptions was made for the dynamics model:

- Thrust and Mass are fixed functions of time. A reference simulation flight is used to simplify these variables.
- Axial forces acting on the rocket include thrust, drag, and airbrake drag.
- Coefficients of axial force and drag are obtained as fixed functions of Mach at low angles of attack (less than 10 degrees).
- Normal forces and torques acting on the rocket include wind-disturbance and act at the center-of-pressure.
- Aerodynamic stability is disregarded to simplify the simulation. Further aerodynamic effects will be considered in a later version.

Therefore, we consider the following 1-dimensional non-linear, time-varying system.

$$\dot{x} = f(x, u) + w \quad (3)$$

Where $f(*)$ denotes the nominal model of the dynamics, $x_k = [Z \ V \ \Omega \ L]$ denotes the state vector of the system, $u = F_a$ denotes the airbrake fin projection angle as the control input, and w represents the wind-disturbance. The control input u is computed using a simplified bluff-body flat plate approximation ($C_d = 1.28$). The equation for the axial component of the airbrake system during simulation is computed as follows:

$$F_a = \frac{1}{2} \rho v^2 C_d A \sin(u) \quad (4)$$

B. Wind Disturbances

While aerodynamic stability effects are not considered, the wind-disturbance adds noise to the lateral and rotational dynamics of the rocket in flight. Wind velocity is sampled from a gaussian distribution centered around a mean wind-velocity at each simulation timestep. The wind force is computed using the projected area of the rocket multiplied by the induced dynamic pressure.

evaluating simple or complex shapes. A graph of this is presented in Fig. 8 on the following page for both the brakeless rocket and vehicle with full airbrake deployment to compare the range of C_d s that will be experienced during flight. These values were again calculated using atmospheric conditions at 4,000 feet, resulting in a speed of sound value of 1100.99 ft/s for Mach number calculations.

V. Flight Simulation

A high-powered rocket's trajectory consists of powered and coasting phases. The rocket begins at rest on the launchpad with an initial state X_0 and continues until motor burnout. During powered ascent, the airbrake system remains inactive to prevent flight instability. After burnout, the coasting phase begins, and the airbrake system gains control authority over the flight. The rocket coasts to the final state of flight, apogee (X_f).

To evaluate airbrake performance, a

C. Optimal Path Planning

To analyze the trajectory of the airbrake system, a best-case control scenario can be computed using the standard optimal control problem.³ We formulate a minimum-energy optimal control problem with the goal of reaching the target apogee within specified constraints. The cost function considers the deviation of the rocket from the target altitude and a terminal constraint of reaching the target apogee. The full quadratic objective function can be found below.

$$J(x, u) = \int_0^T (X_{target} - X)^T Q (X_{target} - X) dt + P^T u \quad (5)$$

Where Q and P are positive-definite weight matrices. Constraints are defined on the airbrake control input to limit the amount of extension on the airbrake surfaces. To solve the optimal control problem, a minimizer is used to compute the control input to the system simulation.

VI. Results

A. Simulated Flight-Performance Data

Two simulations were performed using the parameters of the L2 rocket shown above. The first experiment consisted of analyzing the open-loop response of the dynamics model. All initial conditions were set to zero except the roll and yaw angles were set to 4 degrees to mimic an actual launch setup into the wind. While it is understood that the neglect of aerodynamic stability causes inaccuracies in response to disturbances, an accurate apogee altitude was achieved with respect to the Ras Aero II simulation of the L2 rocket. The results of this analysis are shown in Fig 9.

The rocket achieves an apogee altitude of 4,394 feet with a downrange distance of 133.2 feet. Next, the closed-loop response with an optimal controller was simulated. A target apogee of 3500 feet was selected to study the feasibility of a large change in altitude induced by the airbrake system. The results of this analysis are shown in Fig 10.

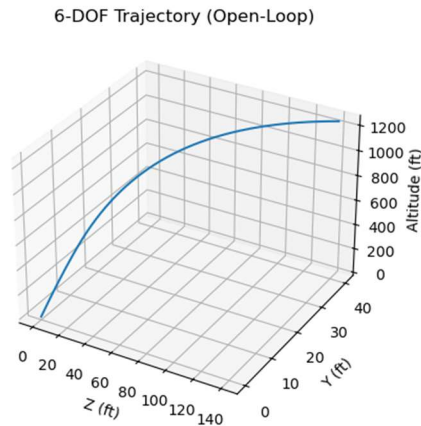


Figure 11. Position of the rocket during flight.

6-DOF Trajectory (Closed-Loop)

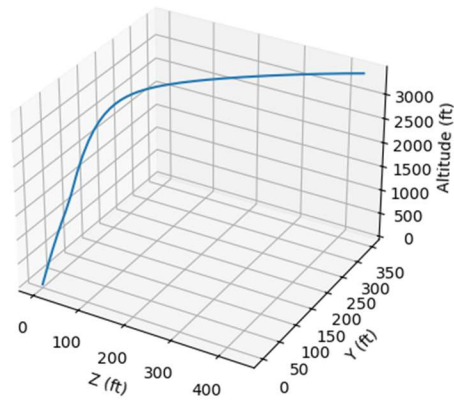


Figure 10. Position of the rocket during controlled flight.

The rocket achieves a target apogee of 3500 feet with a downrange distance of 531 feet. The results of this analysis show a tradeoff between the apogee and downrange distance. The optimal controller can control the airbrake system even at a large, desired change in apogee of the rocket.

VII. Aerodynamic Data

There are slight differences between the drag forces calculated via hand calculations and CFD simulations, giving an envelope from which we can expect the actual flight forces to fall within. The rocket itself is calculated to experience a drag difference of 5.4% in the CFD and analytical calculation. The airbrake fins have more variance between the two methods, with 17.0 lbf with hand calculations vs. 11.4 lbf in CFD. One reason this difference is relatively large could be due to the 1.28 C_d used for flat plate

analysis, compared to the CFD model simulating the entire vehicle and the largest C_d value being .7053. These results are in the same ballpark as what RAS Aero is outputting, which is the software primarily used for Space Cowboys rocket development. The program indicates 32 lbf of drag on the vehicle, compared to 31.9 lbf total for the CFD model (0.3% difference) and 36.4 lbf for the hand calculated program (13.8% difference).

Referring to the CFD discussion earlier in the paper, the variance between the drag during full deployment and no deployment is the purple line in Fig. 7. This is the amount of drag induced by the airbrakes alone, and with some quadratic regression used to get a best fit line as follows:

$$F_D = 0.00002v^2 + 0.0004v - 0.0344 \quad (6)$$

Integrating this equation with an upper bound of maximum velocity (velocity at motor burnout) of 578 ft/s and lower bound of 0 (at apogee), 1334.27 lbf-ft/s of power is “available” for the rocket to use on its ascent if the airbrakes were fully deployed from motor burnout to apogee.

VIII. Conclusion

Designing and simulating a rocket that can hit a specific target apogee is a difficult process. An active control system such as airbrakes can enable greater precision and account for a larger variability in performance from flight simulations. The airbrake system developed in this project will assist in the development of a potential system for Space Cowboys’ 2024-2025 rocket. This initial prototype consists of a 4-fin mechanism that deploys drag-inducing surfaces normal to the airframe. The fins are precisely controlled via a single servo motor paired with a low-latency control system that can adjust the fin-extension during the rocket’s flight while referencing pre-computed trajectory values. In this report, we have validated the mechanism works as designed and verified that the drag surfaces can significantly alter a rocket’s apogee.

While the team was ultimately not able to complete any wind tunnel testing as planned due to an inoperable wind tunnel at the university, testing can be planned and completed for future quantitative data once it comes back online. Additional tests under consideration are flight tests and drop tests. Once the Level 2 rocket that this system was designed to fit is completed, the team is looking to fly two initial flights – one with the airbrakes integrated but not used for altitude adjustment and another with the system fully functioning. This will allow the first flight to be a “normal” flight and for the data between the two flights a direct comparison to visualize the outcome of the additional drag induced during flight.

For the drop tests, a test object with the airbrakes integrated can be physically dropped from an adequate height for the assembly to reach terminal velocity. At terminal velocity, the forces of gravity equal the forces of air resistance and therefore with all other variables known, the drag force can be determined. Again, multiple tests with various deployment stages can be tested to get a full idea of the range of additional drag forces that can be added. While dropping a full-scale rocket would be ideal, the aerodynamic efficiency of a rocket would make terminal velocity quite high and require the drop from a tall height. Therefore, since the data we would be looking for is just the added drag from fins, a simpler geometry and lighter mass housing for the system would be ideal.

The airbrake simulation software will be further refined to support a Monte-Carlo analysis of the rocket in response to additional flight disturbances, such as uncertainty in aerodynamic parameters. A more robust approach to wind modeling will also be considered, considering varying windspeeds at altitude. The potential for a more robust optimal control method will also be explored. We understand that our assumption on aerodynamic stability effects greatly affects the accuracy of our simulation, and we hope to address this in future versions.

Ultimately, the research done by this project will be concluded with integration and multiple flight tests done in the Space Cowboys’ competition rocket in future school years. The team is confident that the work done here using a Level 2 NAR certification rocket will scale to any size diameter airframe that the team works with, with minimal adjustments to internal mechanisms and fin design.

IX. References

- ¹Box, S., Bishop, C. M., & Hunt, H. (2010). A stochastic six-degree-of-freedom flight simulator for passively controlled high-power rockets. *Journal of Aerospace Engineering*, 24, 31-45. DOI: [10.1061/ASCEAS.1943-5525.0000051](https://doi.org/10.1061/ASCEAS.1943-5525.0000051)
- ²J. Compos. Sci. 2021, 5, 147. <https://doi.org/10.3390/jcs5060147>
- ³Lew, T., Lyck, F., & Müller, G. (2019). Chance-Constrained Optimal Altitude Control of a Rocket. In *8th European Conference for Aeronautics and Aerospace Sciences (EUCASS)* (pp. 1-15). DOI: [10.13009/EUCASS2019-388](https://doi.org/10.13009/EUCASS2019-388)
- ⁴Rocket Stability. NASA. [https://doi.org/10.1061/\(ASCE\)AS.1943-5525.0000051](https://doi.org/10.1061/(ASCE)AS.1943-5525.0000051)
- ⁵RocketPy — RocketPy 1.0.1 documentation.
- ⁶NASA Glenn Research Center. "Airfoil Shape." Virtual Aerospace Engineering - Bottle Rocket, 2004, <https://www.grc.nasa.gov/www/k-12/VirtualAero/BottleRocket/airplane/shaped.html#:~:text=A%20flat%20plate%20has%20Cd,5%2C%20a%20bullet%20Cd%20%3D%20>.
- ⁷MATLAB, Matrix Laboratory, Software Package, Ver. R2022b, The MathWorks Inc., Natick, MA, USA, 2022.
- ⁸OpenRocket, Software Package, Ver. 23.09, Open Source, 2023.
- ⁹RAS Aero II, Software Package, Ver. 1.0.2.0, Rogers C.E. and Cooper D., 2019.
- ¹⁰SolidWorks, Software Package, Ver. 2023, Dassault Systems, Vélizy-Villacoublay, France, 2023.
- ¹¹Van Milligan T., "How to Determine the Drag Coefficient of Your Rockets," *Peak of Flight Newsletter*, Issue 303, Apogee Components, URL: <https://www.apogeerockets.com/education/downloads/Newsletter303.pdf> [cited 3 January, 2012].
- ¹²Aaron III, R.F., "Altitude-Limiting Airbrake System for Small-Medium Scale Rockets," *NASA Technical Reports Server* [online database], URL: <https://ntrs.nasa.gov/api/citations/20140013095/downloads/20140013095.pdf> [cited 20 December 2013].

IX. Appendix

A. CFD Results

A1. Brakeless Rocket (0% Fin Deployment)

Velocity (ft/s)	F _d (lbf)	C _d
0	0	0
82.025	0.2738	0.4554
164.050	1.1315	0.4705
246.075	2.4684	0.4562
328.100	4.2938	0.4464
410.125	6.6012	0.4392
492.150	9.3855	0.4337
574.175	12.5971	0.4276
656.200	16.3470	0.4249
738.225	20.4817	0.4206

A2. 100% Fin Deployment

Velocity (ft/s)	F _d (lbf)	C _d
0	0	0
82.025	0.4167	0.6932
164.050	1.6960	0.7053
246.075	3.7457	0.6923
328.100	6.5668	0.6827
410.125	10.1775	0.6772
492.150	14.5816	0.6738
574.175	19.6894	0.6684
656.200	25.4868	0.6624
738.225	31.9033	0.6552

A3. 75% Fin Deployment

Velocity (ft/s)	F _d (lbf)	C _d
0	0	0
82.025	0.3499	0.5820
164.050	1.4302	0.5948
246.075	3.1445	0.5812
328.100	5.5006	0.5719
410.125	8.5316	0.5677
492.150	12.2007	0.5637
574.175	16.4946	0.5599
656.200	21.4077	0.5564
738.225	26.8231	0.5508

A4. 50% Fin Deployment

Velocity (ft/s)	F _d (lbf)	C _d
0	0	0
82.025	0.2740	0.4558
164.050	1.1363	0.4725
246.075	2.4830	0.4589
328.100	4.3191	0.4490
410.125	6.6374	0.4416
492.150	9.4511	0.4367
574.175	12.7094	0.4312
656.200	16.4473	0.4275
738.225	20.5959	0.4230

A5. 25% Fin Deployment

Velocity (ft/s)	F _d (lbf)	C _d
0	0	0
82.025	0.2658	0.4421
164.050	1.1072	0.4604
246.075	2.4081	0.4451
328.100	4.1856	0.4351
410.125	6.4878	0.4317
492.150	9.2768	0.4286
574.175	12.4746	0.4235
656.200	16.2790	0.4231
738.225	20.4567	0.4201

B. Dynamics Model Equations

$$\dot{\mathbf{r}} = \mathbf{C}_{I-B}(t) * \mathbf{v}_b \quad (7)$$

$$\dot{\mathbf{v}}_B = \frac{(\mathbf{T}_B(t) + \mathbf{A}_B(M) + \mathbf{U}_{AB})}{m(t)} + \mathbf{g}_B - (\boldsymbol{\omega}_B \times \mathbf{v}_B) \quad (8)$$

$$\dot{\boldsymbol{\Omega}} = \mathbf{E}_{I-B}(t) * \boldsymbol{\omega}_B \quad (9)$$

$$\dot{\boldsymbol{\omega}}_B = \check{\mathbf{J}}_B^{-1}[\mathbf{R}_{T,B} \times \mathbf{T}_{\omega,B} + \mathbf{R}_{CP,B} \times \mathbf{A}_B(m) + \mathbf{R}_{F,B} \times \mathbf{U}_{AB,B}] - \check{\mathbf{J}}_B^{-1}(\boldsymbol{\omega}_B \times \check{\mathbf{J}}_B * \boldsymbol{\omega}_B) \quad (10)$$